

Probing a minimal dark gauge sector via microlensing of compact dark objects

Juan Barranco,¹ Argelia Bernal,^{1,2} Víctor Jaramillo,³ Darío Núñez,⁴ and Milton Ruiz⁵

¹*Departamento de Física, División de Ciencias e Ingenierías,
Campus León, Universidad de Guanajuato, C.P. 37150, León, México*

²*Instituto de Física y Matemáticas, Universidad Michoacana de San Nicolás de Hidalgo,
Edificio C-3, Ciudad Universitaria, 58040 Morelia, Michoacán, México*

³*Department of Modern Physics, University of Science and Technology of China, Hefei, Anhui 230026, China*

⁴*Instituto de Ciencias Nucleares, Universidad Nacional Autónoma de México,
Circuito Exterior C.U., A.P. 70-543, Coyoacán, México 04510, CdMx, México*

⁵*Departament d'Astronomia i Astrofísica, Universitat de València,
C/ Dr Moliner 50, 46100, Burjassot (València), Spain*

(Dated: February 26, 2026)

We introduce a minimal Dark Standard Model (DSM) consisting of a single spin-0 particle with dark $U(1)$ gauge symmetry, and completely decoupled from the visible sector. Characterized only by the scalar mass μ and the dark charge q , this framework naturally gives rise to a rich phenomenology, including stable solitonic configurations that behave as dark “mini-MACHOs”. We numerically build and evolve these gauged scalar-field solitons, derive their mass-radius relations, and identify a critical charge beyond which no gravitationally bound configurations exist. By combining these results with microlensing surveys that exclude compact objects heavier than the asteroid-mass scale ($M \lesssim 10^{-11} M_\odot$), we obtain the constraint $\mu \gtrsim 10$ eV for viable configurations, depending on q . Our results represent a step forward in showing that purely gravitational observations can constrain the internal parameters of a dark gauge sector, and provide a framework for exploring broader DSM scenarios through future probes such as gravitational wave detections.

I. INTRODUCTION

The discovery of dark matter (DM) through its gravitational interaction with visible matter has been confirmed at galactic [1–4] and cosmological scales [5–11]. The compelling evidence for the existence of dark matter has driven the development of terrestrial experiments pursuing its direct or indirect detection [12, 13]. Terrestrial experimental searches need to assume a coupling of the DM candidate to visible matter beyond a pure gravitational interaction in order to get a detection signal. While this experimental approach may eventually detect dark matter, current observations imply that there is no empirical evidence that DM couples with standard model (SM) particles [14–24]. In this scenario, an even more elusive possibility arises: that multiple dark matter particles could exist, none of them coupled to those of the SM.

We explore the possibility that dark matter may be composed of distinct particle fields preserving local gauge symmetries, mediated by their own gauge mediators, in analogy with the Standard Model (SM). These fields are minimally coupled to gravity but fully decoupled from SM. We refer to this scenario as the Dark Standard Model, DSM. If such DSM exists, several questions arise: i) what is its particle content?; ii) What gauge symmetries dictate the dynamics of DM interactions?; and, most challenging, iii) how could we experimentally probe the DSM and its associated dark symmetries? As a step forward in addressing these questions, we consider a minimal realization of the DSM consisting of a spin-0 particle with an internal $U(1)$ gauge symmetry. This represents a textbook example of a gauge theory that has the lowest number of free parameters: the scalar mass μ and the charge q .

Despite having only two parameters, this DSM has a rich phenomenology. For instance, when $q = 0$ and for

masses μ of the order of 10^{-22} eV, the model reduces to the Scalar Field Dark Matter (SFDM) scenario, also known as Fuzzy Dark Matter Model, which successfully reproduces the Cold Dark Matter (CDM) at cosmological scales and, at galactic scales, and may alleviate small-scale (central halo regions) CDM tensions [25, 26].

While the SFDM scenario focuses on wave-like dark matter behavior, scalar fields can also behave as particle-like, compact configurations. In this scenario, they can also be used within the CDM model, which considers that dark matter is composed of non-interactive particles [27], and these particles can be regarded as scalar-field objects. Moreover, microlensing studies [28–30] imply that, if the galactic halos are composed of clusters of massive objects, they cannot have a mass larger than $10^{-11} M_\odot$, often referred to as mini-MACHOs. Previous studies with scalar field compact objects (see e.g. [31–33]) showed that galactic halos could be modeled as collisionless ensembles of scalar field MACHOs with masses below than $10^{-7} M_\odot$, which was the upper limit at that time.

Within this point of view, we show that for $\mu \simeq 1$ eV, self-gravitating scalar field configurations have masses around $10^{-11} M_\odot$ and can play the role of massive compact halo objects (MACHOs). In such a scenario, the halo dynamics would be indistinguishable from that in a CDM halo, since N-body simulations of CDM are insensitive to particle mass granularity smaller than $10^5 M_\odot$ [27]. These scalar field mini-MACHOs could have formed in the early Universe via a mechanism analogous to the Affleck-Dine Mechanism known in particle physics [34]. Dark neutron stars have recently been investigated within a related framework [35], while Ref. [36] analyzes gravitational microlensing by a class of static, spherically symmetric nonsingular black holes. Related Higgs-portal constructions with a spontaneously broken global $U(1)$ symmetry have also been explored [37]. More recently, it has been shown that nonminimal couplings to

gravity may produce demagnification signatures in microlensing light curves [38].

Static, spherically symmetric, self-gravitating systems minimally coupled to a scalar field with $U(1)$ gauge symmetry, known as charged boson stars, have been described in [39–42]. Recently, the dynamics of these self-gravitating configurations was studied in [43]. In this work, we reinterpret these configurations as dark matter structures within the DSM framework. The resulting solutions are everywhere regular and horizonless, representing solitonic equilibria of the model. In contrast, black hole configurations with nontrivial scalar field profiles exist only for self-interacting scalars under specific resonance conditions [44, 45]. Such solutions can be continuously connected to the self-interacting (Q-ball-like) boson star sequence when a small event horizon is introduced. However, full 3+1 numerical evolutions show that they develop a non-axisymmetric instability [46], while their horizonless counterparts remain stable [43]. Therefore, within this theory, the viable static gravitational solitons that could serve as MACHO dark matter candidates are the Reissner–Nordström black holes and the gauged boson stars. Throughout the paper we adopt geometric units ($c = 1 = G$) except where stated otherwise. In these units, the coupling parameter q then has units of inverse length and can be normalized by the scalar field mass μ , so that ratio q/μ becomes dimensionless.

II. GAUGE DARK MATTER SOLITONS

The action for the minimal DSM model is

$$S = \int d^4x \sqrt{-g} \left[\frac{1}{16\pi} R - g^{\alpha\nu} \mathcal{D}_\alpha \Phi \mathcal{D}_\nu \Phi^* - \mu^2 |\Phi|^2 - \frac{1}{4} F_{\alpha\nu} F^{\alpha\nu} \right], \quad (1)$$

where μ is the mass of the spin-0 particle, $F_{\alpha\nu} = \partial_\alpha A_\nu - \partial_\nu A_\alpha$, $g_{\alpha\nu}$ is the spacetime metric, R the Ricci scalar. Here A_ν is the four-potential. Notice that we use the gauge invariant covariant derivative operator defined as $\mathcal{D}_\alpha = \nabla_\alpha + i q A_\alpha$, where q is the gauge coupling constant or the scalar field charge [43].

Variation with respect to $g_{\alpha\nu}$ leads to the Einstein field equations, with the stress energy tensor given by

$$T_{\alpha\nu} = 2\mathcal{D}_\alpha \Phi \mathcal{D}_\nu \Phi^* - g_{\alpha\nu} (\mathcal{D}^\beta \Phi \mathcal{D}_\beta \Phi^* + \mu^2 |\Phi|^2) + F_{\alpha\sigma} F_{\nu\lambda} g^{\sigma\lambda} - \frac{1}{4} g_{\alpha\nu} F_{\sigma\beta} F^{\sigma\beta}. \quad (2)$$

Variation with respect to A_α leads to the Maxwell equations sourced by the spin-0 current J^α ,

$$\nabla_\nu F^{\alpha\nu} = J^\alpha := q J_\Phi^\alpha, \quad (3a)$$

$$J_\Phi^\alpha := i (\Phi^* \mathcal{D}^\alpha \Phi - \Phi \mathcal{D}^\alpha \Phi^*), \quad (3b)$$

here J_Φ^α is the conserved current that arises from the $U(1)$ gauge invariance of Eq. (1). Finally, variation with respect Φ leads to the Klein-Gordon equation

$$\mathcal{D}^\alpha \mathcal{D}_\alpha \Phi = \mu^2 \Phi. \quad (4)$$

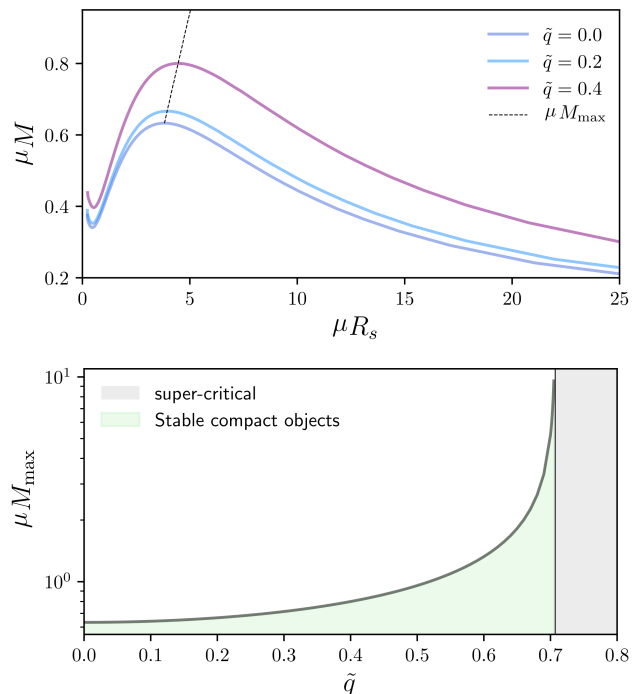


FIG. 1. Gauge dark matter solitons sequence of solutions. Top panel: Mass vs. radius diagram for families of configurations with different values of q . Dashed-line displays the maximum mass configurations. Lower panel: Maximum mass configuration as a function of q in the region where gravitationally bound, and stable configurations exist. Beyond the critical $\tilde{q}_{\text{crit}} = 1/\sqrt{2} \approx 0.707$, no gravitationally bound solutions are found.

The minimal energy, self-gravitating realization of model in Eq. (1) is a static spherically symmetric spacetime with a stationary scalar field spherical solutions,¹ characterized by a harmonic time dependence of the scalar field of the form $\Phi = \phi(r)e^{i\omega t}$ and an “electric” potential $A_\alpha dx^\alpha = V(r)dt$. We choose coordinates in which the spacetime metric takes the form

$$ds^2 = -e^{2F_0(r)} dt^2 + e^{2F_1(r)} (dr^2 + r^2 d\Omega^2), \quad (5)$$

with $d\Omega^2 = d\theta^2 + r^2 \sin^2 \theta d\varphi^2$ the solid angle. Notice that the metric is isotropic.

Under these assumptions for the spacetime and the spin-0 and spin-1 fields, the system reduces to four coupled ordinary differential equations for the functions $V(r)$, $\phi(r)$, $F_0(r)$ and $F_1(r)$, see e.g. Appendix B in [43] (or [47] for a more general treatment in a non-relativistic limit). We solve the system numerically, noting first that the mass of the scalar field μ can be factored out as the characteristic length scale of the system, and all dimensional quantities rescale with appropriate powers μ . We solve the system using a spectral method with a compactified radial coordinate r and a Newton-Raphson algorithm, as described in [48], and employ 24 spectral coefficients for all solutions presented. In the process,

¹ Often referred as charged boson stars (see e.g. [39]).

TABLE I. Gauge dark matter solitons: configurations of maximum mass as a function of the rescaled coupling \tilde{q} . We list the dimensionless rescaled charge \tilde{q} , the eigenfrequency frequency of the the spin-0 field ω , the maximum value of the scalar field at the origin $\phi(r=0)$, the mass μM , the total electrical charge μQ_E , and the radius μR_s of the configurations. The critical value $\tilde{q}_{\text{crit}} = 1/\sqrt{2} \approx 0.707$ marks the limit beyond which no gravitationally bound solutions exist.

\tilde{q}	ω/μ	$\phi(r=0)$	μM	μQ_E	μR_s
0	0.8530	0.0765	0.6330	0	3.816
0.7	0.9958	0.0158	5.203	30.96	22.86
0.705	0.9987	0.00871	9.567	57.69	41.71

the eigenfrequency of the the spin-0 field ω is determined as part of the solution. The equilibrium configurations obtained in this scenario form sequences characterized by the coupling constant q , which has an upper bound of approximately $q = \sqrt{4\pi\mu}$ that is limited by Coulomb repulsion [39, 41, 42, 49–51]. Following previous literature [39, 42], we present results in terms of the dimensionless rescaled charge $\tilde{q} = q/(\sqrt{8\pi\mu})$, for which the critical value is $\tilde{q}_{\text{crit}} = 1/\sqrt{2}$. For the solitons considered here, the central amplitude of the scalar field parametrizes each sequence of solutions. The top panel of Fig. 1 shows some sequences for several values of q . Here M denotes to the total mass of the configuration, obtained from the asymptotic behavior of the metric coefficients:

$$M = - \lim_{r \rightarrow \infty} \left(r^2 \frac{dF_1}{dr} \right), \quad (6)$$

from the g_{rr} component, or

$$M = \lim_{r \rightarrow \infty} \left(r^2 \frac{dF_0}{dr} \right), \quad (7)$$

from the g_{tt} component. Both should coincide and we use this two quantities to asses accuracy of the code. The first definition corresponding to the Arnowitt–Deser–Misner (ADM) mass, while the second corresponds to the Komar mass (see e.g. [49, 52, 53]). Following [48], the radius of the configuration is defined as the areal radius R where $C := M(R)/R = e^{-F_1} M(r)/r$ is maximized. Here $M(r)$ denotes the Misner-Sharp function, which in isotropic coordinates is $M(r) = -r^2 e^{F_1} \partial_r F_1 (1 + r \partial_r F_1 / 2)$. The conserved charge Q associated with the conserved current J_α^a in Eq. (3b), is given by

$$Q = 4\pi \int_0^\infty e^{3F_1 - F_0} r^2 \phi^2 (Vq + \omega) dr, \quad (8)$$

which is related to the total “electrical” charge Q_E of the soliton through $Q_E = qQ$. Far from the source, the electric potential decays as

$$V(r) = -\frac{Q_E}{4\pi r} + \mathcal{O}\left(\frac{1}{r^2}\right), \quad (9)$$

which we again use to check accuracy of our numerical solutions. We have checked that the relative differences

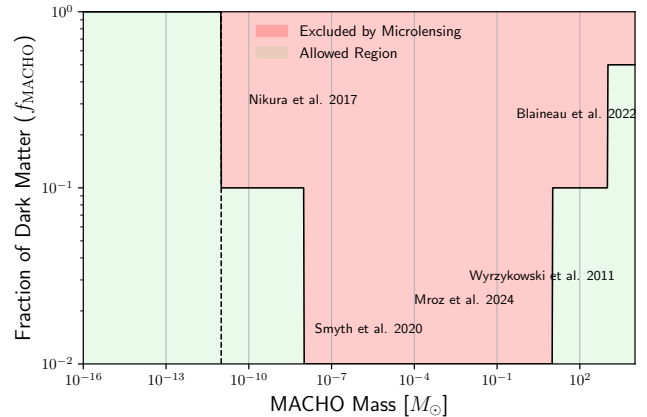


FIG. 2. Summary of current microlensing limits on the MACHO dark matter fraction as a function of lens mass. The solid black line marks the combined 95% confidence level exclusion boundary obtained from recent surveys. Nikura et al. [54] constrain the sub-lunar window around $10^{-11} - 10^{-6} M_\odot$, Smyth et al. [55] probe the Earth–Jupiter range $10^{-6} - 10^{-3} M_\odot$, Wyrzykowski et al. [56] constrain the stellar regime $\sim 10^{-1} - 10 M_\odot$, and Blaineau et al. [57] cover the intermediate range $10 - 10^3 M_\odot$. Updated OGLE analyses combining the results of Refs. [58, 59] further impose global limits, excluding MACHOs contributing more than 1% of the dark matter in the mass range $10^{-8} - 10 M_\odot$, and more than 10% in the broader interval $10^{-9} - 10^3 M_\odot$. The red-shaded regions above the exclusion boundary are therefore ruled out.

between the ADM and Komar masses, as well as between the two charge definitions, are below 10^{-4} .

Note that the total charge Q has no definite sign, as it depends on the product of the gauge coupling q , which is fixed in sign, and ω , which can be either positive or negative. The Maxwell Eqs. given by Eq. (3) is invariant under $(\omega, A_\alpha) \rightarrow (-\omega, -A_\alpha)$, implying that once the parameter q is fixed, a change in the sign of ω reverses the total electrical charge, as seen from Eq. (8).

Fig. 1 shows that, for each value of q , there is a maximum value of M (dashed-line in the top panel) that increases with q . Table I lists additional properties of the corresponding dark-matter solitons, including their radius R_s , and total charge Q_E . Stability analysis, both perturbative [40] and non-perturbative [42, 43], have concluded that, configurations with radii larger than that of the maximum mass configurations are stable. Therefore, all configurations on the right side of the maximum (see top panel of Fig. 1) remain stable, while those to the left side are unstable: they either collapse to a black hole, relax into a lower-mass equilibrium state, or disperse. The lower panel of Fig. 1 shows M_{max} as a function of the coupling parameter q in the range $[0, 0.705]$. Configurations beyond the critical charge value $\tilde{q}_{\text{crit}} = 1/\sqrt{2} \approx 0.707$ were found to be gravitationally unbound and therefore unstable. In summary, for each value of q , there exist a sequence of solutions. If $q < q_{\text{crit}}$, a global maximum-mass configuration separates the stable from the unstable branch. These numerical results constrain the dimensionless quantity μM as function of q (see lower panel of Fig. 1).

In the next section, we use microlensing limits on MA-

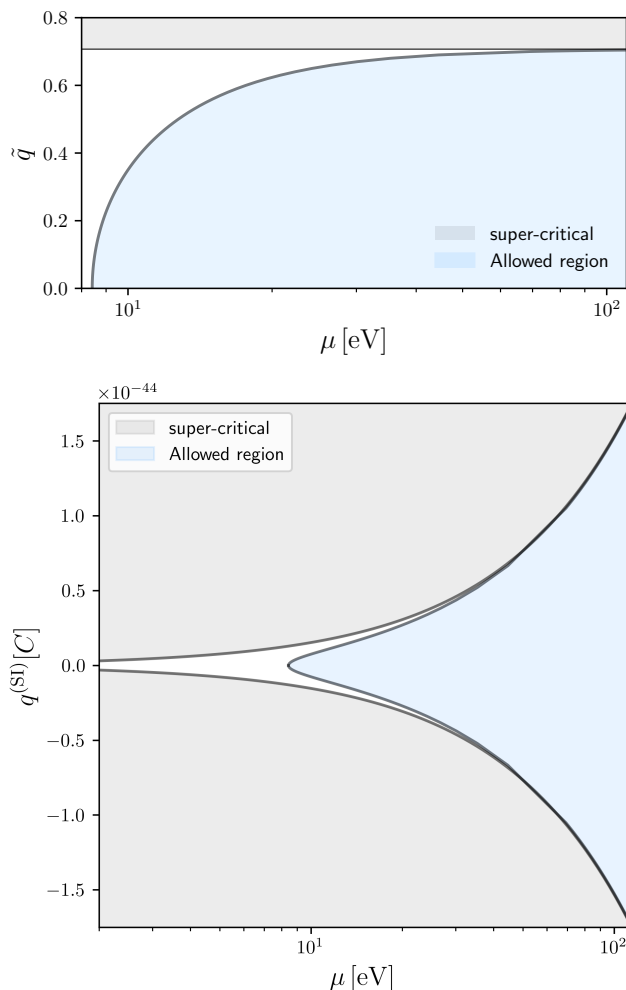


FIG. 3. Constraints in the plane (μ, q) parameter space derived from the non-observation of microlensing events. The shaded region indicates the values of the scalar-field mass μ and coupling q consistent with current MACHO limits. Larger masses are excluded by Eq. (11).

CHOs to further constrain the allowed values of M , and consequently the parameters μ and q .

III. CONSTRAINTS ON THE FREE μ AND q FROM MICROLENSING LIMITS

Current microlensing observations have imposed tight constraints on the fraction of dark matter that may be due to MACHOs. As summarized in Fig. 2, these limits depend on the mass of the compact objects \mathcal{M} . Microlensing observations have effectively excluded MACHOs with $\mathcal{M} > 10^{-11} M_\odot$ as the dominant dark matter. In the sub-lunar to Earth-mass range ($10^{-11} \lesssim \mathcal{M}/M_\odot \lesssim 10^{-6}$), the Subaru Hyper Suprime-Cam (HSC) survey of M31 by Niikura et al. [54] detected only one candidate event, placing strong upper limits on the MACHO fraction of dark matter and effectively closing the so-called “lunar-mass window”. At lower masses ($10^{-16} \lesssim \mathcal{M}/M_\odot \lesssim 10^{-10}$), Smyth et al. [55] reanalyzed the same HSC data, incorporating finite-source-size effects. They

found that these effects significantly weaken constraints at the smallest masses, suggesting that asteroid-mass MACHOs could still constitute all of the dark matter. At solar masses and above, OGLE observations toward the Magellanic Clouds, particularly those by Wyrzykowski et al. [56], show that the detected microlensing events are consistent with known stellar populations, thereby ruling out MACHOs with $\mathcal{M} \sim 0.1 - 10 M_\odot$ as more than a small fraction of the dark halo. For heavier objects in the intermediate range ($\mathcal{M} \sim 10 - 10^3 M_\odot$), Blaineau et al. [57] combined MACHO and EROS datasets, finding that such black hole-like MACHOs can account for at most about 15%–50% of the dark matter, depending on mass. Overall, microlensing surveys have largely ruled out MACHOs as the dominant form of dark matter, leaving room primarily for mini-MACHOs in the asteroid-mass regime.

We model MACHOs using the gauge dark matter solitons described in the previous section and show how microlensing limits constrain the parameters μ and q . For a fixed q , we numerically obtain a maximum value of μM , a consequence of the self-gravitating nature of the solitons in the minimal gauge dark matter mode in Eq. (1) [60].

From the above observational constraints, MACHO masses must satisfy

$$\mathcal{M} \lesssim 10^{-11} M_\odot = 1.48 \times 10^{-8} \text{m}. \quad (10)$$

Therefore, we require that the maximum mass of the solitonic configurations in Eq.(1) not exceed this bound, i.e.

$$M_{\text{max}} < 1.48 \times 10^{-8} \text{m}. \quad (11)$$

Otherwise, stable solutions exceeding this bound would have masses already ruled out by current microlensing limits. This condition imposes a constraint on the scalar-field mass μ :

$$\mu > 6.76 \times 10^7 x(q) \text{m}^{-1} = 13.3x(q)\text{eV} \quad (12)$$

where $x(q) = \mu M_{\text{max}}$ is obtained from the numerical sequences shown in the lower panel of Fig. 1, or from some specific configurations in Table I. The corresponding constraints on μ as function of q are displayed in the top panel of Fig. 3. In the lower panel, we also show the resulting allowed region with the coupling constant given in SI units, using the conversion

$$q^{(SI)} = \frac{\sqrt{8\pi G\hbar}}{c^2 \sqrt{\mu_0}} \mu \tilde{q} = 2.167 \times 10^{-46} \left(\frac{\mu}{\text{eV}} \right) \tilde{q} C, \quad (13)$$

where G is Newton’s gravitational constant, \hbar the reduced Planck constant, c the speed of light in vacuum, and μ_0 the vacuum permeability.

The above results identify a narrow region in the parameter space where gravitationally bound, stable solitons remain compatible with current microlensing constraints. In particular, microlensing non-detections restrict the dark scalar sector to relatively heavy field masses and small gauge couplings, defining a narrow window of viable mini-MACHO configurations within the DSM framework.

IV. CONCLUSIONS

The dynamics of visible matter on both galactic and cosmological scales have implications for the existence of dark matter through their gravitational interaction. To date, there is no experimental evidence that dark matter interacts with visible matter through any force other than gravity. However, it is possible that the dark matter sector is not composed of a single particle, but instead forms a self-consistent dark analogue of the Standard Model with its own gauge interactions.

We introduced a minimal Dark Standard Model with a dark $U(1)$ gauge symmetry, giving rise to solitonic “mini-MACHOs.” We have presented this scalar field model not as fuzzy dark matter, but within the CDM framework, where dark matter consists of non-interactive particles. We showed that these particles could be composed of a scalar field, whose rest mass must be greater than 10 eV, with more restrictive constraints for a non-zero dark charge.

By combining our derived mass-radius relations for these solitons with microlensing constraints on asteroid-mass objects, we obtain a lower bound of $\gtrsim 10$ eV on the scalar mass μ . We derived this bound from the non-observation of microlensing events, combined with the general properties of gauged scalar field stars. Our main results are summarized in Fig. 3, where, for each value of the gauge coupling q , we identify a corresponding minimum allowed scalar-field mass. In particular, for $q = 0$, the bound is of order 10 eV.

From Fig. 3, one may conclude that current microlensing observations impose a lower limit on the scalar-field mass μ , while the gauge coupling q is restricted by the theoretical condition $\tilde{q} < \tilde{q}_{\text{crit}} = 1/\sqrt{2}$, which ensures the existence of gravitationally bound equilibrium configurations. Only sufficiently heavy fields can form compact objects compatible with current surveys. This shifts the viable parameter space of the minimal DSM to μ -values well above the ultralight fuzzy/axion-like regime.

These configurations are everywhere regular and horizonless, forming dynamically stable solitonic equilibria of the model in Eq. (1). In contrast, as mentioned above, black hole counterparts with nontrivial scalar hair arise only in self-interacting theories under specific resonance conditions and are unstable. Therefore, within the considered framework, the viable static gravitational solitons consistent with current astrophysical constraints are the Reissner–Nordström black holes and the gauged boson stars, the latter standing as natural, stable MACHO

dark matter candidates. The limits we have derived on the scalar field mass could also be affected by considering additional terms in the scalar potential, such as a self-interaction.

The dark matter model proposed in this work also opens new directions for exploring its potential observational signatures. Collisions or mergers of these dark asteroids could contribute to a stochastic gravitational wave background with distinctive spectral features, as discussed previously (see e.g. [61–65]). Furthermore, the accretion of such dark compact objects onto black holes could endow Reissner–Nordström and Kerr–Newman geometries with an effective dark charge, providing a novel physical interpretation of the charge parameter in these solutions. This perspective could be applied in other contexts where the conventional view has been used, such as to matter in the vicinity of black holes. This possibility motivates further studies of geodesic motion and observable effects in such spacetimes, following the approaches developed in [66–68].

Within this scenario, there are multiple other possibilities that can be studied with different gauge mediators and dark matter particles. These bounds are expected to hold in more general dark-gauge sectors with additional fields or interactions. Given the opening of new observational tools and experiments that probe the Universe through gravitational interactions, such as gravitational wave observations, it now seems possible to begin the systematic study of a dark matter standard model along the lines described in this work, potentially connecting gravitational phenomena to the internal structure of the dark sector.

ACKNOWLEDGMENTS

This work has been partially supported by the National Key R&D Program of China under grant No. 2022YFC2204603, by the Generalitat Valenciana (grants CIDEAGENT/2021/046 and Prometeo CIPROM/2022/49), and by the Spanish Agencia Estatal de Investigación (grants PID2024-159689NB-C21 funded by MCIN/AEI/10.13039/501100011033, PRE2019-087617, and ERDF A way of making Europe). We acknowledge computational resources and technical sup-925 port of the Spanish Supercomputing Network through the926 use of MareNostrum at the Barcelona Supercomputing Cen-927 ter (AECT-2023-1-0006).

[1] W. J. G. de Blok, Stacy S. McGaugh, Albert Bosma, and Vera C. Rubin, “Mass density profiles of LSB galaxies,” *Astrophys. J. Lett.* **552**, L23–L26 (2001), [arXiv:astro-ph/0103102](#).

[2] Jan T. Kleyna, Mark I. Wilkinson, N. Wyn Evans, and Gerard Gilmore, “Ursa Major: A Missing low-mass CDM halo?” *Astrophys. J. Lett.* **630**, L141–L144 (2005), [arXiv:astro-ph/0507154](#).

[3] Matthew G. Walker, Mario Mateo, Edward W. Olszewski, Rebecca A. Bernstein, Xiao Wang, and Michael

Woodroffe, “Internal kinematics of the fornax dwarf spheroidal galaxy,” *Astron. J.* **131**, 2114–2139 (2006), [Erratum: *Astron. J.* 132, 968–968 (2006)], [arXiv:astro-ph/0511465](#).

[4] G. Battaglia, A. Helmi, E. Tolstoy, M. Irwin, V. Hill, and P. Jablonka, “The kinematic status and mass content of the Sculptor dwarf spheroidal galaxy,” *Astrophys. J. Lett.* **681**, L13 (2008), [arXiv:0802.4220 \[astro-ph\]](#).

[5] D. N. Spergel *et al.* (WMAP), “First year Wilkinson Microwave Anisotropy Probe (WMAP) observations: De-

- termination of cosmological parameters,” *Astrophys. J. Suppl.* **148**, 175–194 (2003), [arXiv:astro-ph/0302209](#).
- [6] G. Hinshaw *et al.* (WMAP), “Nine-Year Wilkinson Microwave Anisotropy Probe (WMAP) Observations: Cosmological Parameter Results,” *Astrophys. J. Suppl.* **208**, 19 (2013), [arXiv:1212.5226 \[astro-ph.CO\]](#).
- [7] N. Aghanim *et al.* (Planck), “Planck 2018 results. VI. Cosmological parameters,” *Astron. Astrophys.* **641**, A6 (2020), [Erratum: *Astron. Astrophys.* 652, C4 (2021)], [arXiv:1807.06209 \[astro-ph.CO\]](#).
- [8] Sigurd Naess *et al.* (ACTPol), “The Atacama Cosmology Telescope: CMB Polarization at $200 < \ell < 9000$,” *JCAP* **10**, 007 (2014), [arXiv:1405.5524 \[astro-ph.CO\]](#).
- [9] T. de Haan *et al.* (SPT), “Cosmological Constraints from Galaxy Clusters in the 2500 square-degree SPT-SZ Survey,” *Astrophys. J.* **832**, 95 (2016), [arXiv:1603.06522 \[astro-ph.CO\]](#).
- [10] K. Lodha *et al.* (DESI), “DESI 2024: Constraints on physics-focused aspects of dark energy using DESI DR1 BAO data,” *Phys. Rev. D* **111**, 023532 (2025), [arXiv:2405.13588 \[astro-ph.CO\]](#).
- [11] M. Abdul Karim *et al.* (DESI), “DESI DR2 Results II: Measurements of Baryon Acoustic Oscillations and Cosmological Constraints,” (2025), [arXiv:2503.14738 \[astro-ph.CO\]](#).
- [12] R. J. Gaitskell, “Direct detection of dark matter,” *Ann. Rev. Nucl. Part. Sci.* **54**, 315–359 (2004).
- [13] Jennifer M. Gaskins, “A review of indirect searches for particle dark matter,” *Contemp. Phys.* **57**, 496–525 (2016), [arXiv:1604.00014 \[astro-ph.HE\]](#).
- [14] Yue Meng *et al.* (PandaX-4T), “Dark Matter Search Results from the PandaX-4T Commissioning Run,” *Phys. Rev. Lett.* **127**, 261802 (2021), [arXiv:2107.13438 \[hep-ex\]](#).
- [15] J. Aalbers *et al.* (LZ), “First Dark Matter Search Results from the LUX-ZEPLIN (LZ) Experiment,” *Phys. Rev. Lett.* **131**, 041002 (2023), [arXiv:2207.03764 \[hep-ex\]](#).
- [16] J. Aalbers *et al.* (LZ), “Dark Matter Search Results from 4.2 Tonne-Years of Exposure of the LUX-ZEPLIN (LZ) Experiment,” (2024), [arXiv:2410.17036 \[hep-ex\]](#).
- [17] E. Aprile *et al.* (XENON), “First Dark Matter Search with Nuclear Recoils from the XENONnT Experiment,” *Phys. Rev. Lett.* **131**, 041003 (2023), [arXiv:2303.14729 \[hep-ex\]](#).
- [18] E. Adams *et al.* (PICO), “Absorption of Fermionic Dark Matter in the PICO-60 C₃F₈ Bubble Chamber,” (2025), [arXiv:2504.13089 \[hep-ex\]](#).
- [19] C. L. Chang *et al.* (TESSERACT), “First Limits on Light Dark Matter Interactions in a Low Threshold Two Channel Athermal Phonon Detector from the TESSERACT Collaboration,” (2025), [arXiv:2503.03683 \[hep-ex\]](#).
- [20] Rahool Kumar Barman, Geneviève Bélanger, Biplob Bhattacharjee, Rohini M. Godbole, and Rhitaja Sengupta, “Is Light Neutralino Thermal Dark Matter in the Phenomenological Minimal Supersymmetric Standard Model Ruled Out?” *Phys. Rev. Lett.* **131**, 011802 (2023), [arXiv:2207.06238 \[hep-ph\]](#).
- [21] Man Ho Chan, Lang Cui, Jun Liu, and Chun Sing Leung, “Ruling out $\sim 100 - 300$ GeV thermal relic annihilating dark matter by radio observation of the Andromeda galaxy,” *Astrophys. J.* **872**, 177 (2019), [arXiv:1901.04638 \[astro-ph.GA\]](#).
- [22] Deheng Song, Kohta Murase, and Ali Kheirandish, “Constraining decaying very heavy dark matter from galaxy clusters with 14 year Fermi-LAT data,” *JCAP* **03**, 024 (2024), [arXiv:2308.00589 \[astro-ph.HE\]](#).
- [23] A. Albert *et al.* (HAWC), “Search for decaying dark matter in the Virgo cluster of galaxies with HAWC,” *Phys. Rev. D* **109**, 043034 (2024), [arXiv:2309.03973 \[astro-ph.HE\]](#).
- [24] Shang Li and Feng Han, “Search for dark matter annihilation to γ -rays from nearby galaxy clusters with Fermi-LAT data,” *Mon. Not. Roy. Astron. Soc.* **539**, 2242–2247 (2025).
- [25] Tonatiuh Matos, Luis A. Ureña López, and Jae-Weon Lee, “Short review of the main achievements of the scalar field, fuzzy, ultralight, wave, BEC dark matter model,” *Front. Astron. Space Sci.* **11**, 1347518 (2024), [arXiv:2312.00254 \[astro-ph.CO\]](#).
- [26] Lam Hui, Jeremiah P. Ostriker, Scott Tremaine, and Edward Witten, “Ultralight scalars as cosmological dark matter,” *Phys. Rev. D* **95**, 043541 (2017), [arXiv:1610.08297 \[astro-ph.CO\]](#).
- [27] Julio F. Navarro, Aaron Ludlow, Volker Springel, Jie Wang, Mark Vogelsberger, Simon D. M. White, Adrian Jenkins, Carlos S. Frenk, and Amina Helmi, “The Diversity and Similarity of Cold Dark Matter Halos,” *Mon. Not. Roy. Astron. Soc.* **402**, 21 (2010), [arXiv:0810.1522 \[astro-ph\]](#).
- [28] Shude Mao, “Astrophysical applications of gravitational microlensing,” *Research in Astronomy and Astrophysics* **12**, 947–972 (2012), [arXiv:1207.3720 \[astro-ph.GA\]](#).
- [29] Mihael Petač, Julien Laval, and Karsten Jedamzik, “Microlensing constraints on clustered primordial black holes,” *Phys. Rev. D* **105**, 083520 (2022), [arXiv:2201.02521 \[astro-ph.CO\]](#).
- [30] C. Alcock *et al.* (MACHO), “The MACHO project: limits on planetary mass dark matter in the galactic halo from gravitational microlensing,” *Astrophys. J.* **471**, 774 (1996), [arXiv:astro-ph/9604176](#).
- [31] Xavier Hernandez, Tonatiuh Matos, Roberto A. Sussman, and Yosef Verbin, “Scalar field mini-machos: A New explanation for galactic dark matter,” *Phys. Rev. D* **70**, 043537 (2004), [arXiv:astro-ph/0407245](#).
- [32] J. Barranco and A. Bernal, “Self-gravitating system made of axions,” *Phys. Rev. D* **83**, 043525 (2011), [arXiv:1001.1769 \[astro-ph.CO\]](#).
- [33] J. Barranco, A. Carrillo Monteverde, and D. Delepine, “Can the dark matter halo be a collisionless ensemble of axion stars?” *Phys. Rev. D* **87**, 103011 (2013), [arXiv:1212.2254 \[astro-ph.CO\]](#).
- [34] S. Kasuya and M. Kawasaki, “Q Ball formation in the gravity mediated SUSY breaking scenario,” *Phys. Rev. D* **62**, 023512 (2000), [arXiv:hep-ph/0002285](#).
- [35] Jacob A. Litterer and João G. Rosa, “Dark neutron stars from a heavy dark sector,” (2025), [arXiv:2511.01984 \[hep-ph\]](#).
- [36] Jens Boos and Hao Hu, “Microlensing of nonsingular black holes at finite size: A ray tracing approach,” *Phys. Rev. D* **113**, 024065 (2026), [arXiv:2510.10282 \[gr-qc\]](#).
- [37] Kin-Wang Ng, Huitzu Tu, and Tzu-Chiang Yuan, “Dark photons as fractional cosmic neutrino masquerader,” *JCAP* **09**, 035 (2014), [arXiv:1406.1993 \[hep-ph\]](#).
- [38] Hong-Yi Zhang, “Demagnifying gravitational lenses as probes of dark matter structures and nonminimal couplings to gravity,” (2025), [arXiv:2510.05575 \[gr-qc\]](#).
- [39] P. Jetzer and J. J. van der Bij, “CHARGED BOSON STARS,” *Phys. Lett. B* **227**, 341–346 (1989).
- [40] P. Jetzer, “Stability of Charged Boson Stars,” *Phys. Lett. B* **231**, 433–438 (1989).
- [41] Daniela Pugliese, Hernando Quevedo, Jorge A. Rueda H., and Remo Ruffini, “On charged boson stars,” *Phys. Rev. D* **88**, 024053 (2013), [arXiv:1305.4241 \[astro-ph.HE\]](#).
- [42] José Damián López and Miguel Alcubierre, “Charged boson stars revisited,” *Gen. Rel. Grav.* **55**, 72 (2023), [arXiv:2303.04066 \[gr-qc\]](#).

- [43] Víctor Jaramillo, Darío Núñez, Milton Ruiz, and Miguel Zilhão, “Full 3D nonlinear dynamics of charged and magnetized boson stars,” *Phys. Rev. D* **111**, 024070 (2025), [arXiv:2411.07284 \[gr-qc\]](#).
- [44] Carlos A. R. Herdeiro and Eugen Radu, “Spherical electro-vacuum black holes with resonant, scalar Q -hair,” *Eur. Phys. J. C* **80**, 390 (2020), [arXiv:2004.00336 \[gr-qc\]](#).
- [45] Jeong-Pyong Hong, Motoo Suzuki, and Masaki Yamada, “Spherically Symmetric Scalar Hair for Charged Black Holes,” *Phys. Rev. Lett.* **125**, 111104 (2020), [arXiv:2004.03148 \[gr-qc\]](#).
- [46] Jordan Nicoules, José Ferreira, Carlos A. R. Herdeiro, Eugen Radu, and Miguel Zilhão, “Splitting the Gravitational Atom: Instabilities of Black Holes with Synchronized/Resonant Hair,” (2025), [arXiv:2509.20450 \[gr-qc\]](#).
- [47] Hong-Yi Zhang, “Unified view of scalar and vector dark matter solitons,” *JHEP* **04**, 174 (2025), [arXiv:2406.05031 \[hep-ph\]](#).
- [48] Miguel Alcubierre, Juan Barranco, Argelia Bernal, Juan Carlos Degollado, Alberto Diez-Tejedor, Víctor Jaramillo, Miguel Megevand, Darío Núñez, and Olivier Sarbach, “Extreme ℓ -boson stars,” *Class. Quant. Grav.* **39**, 094001 (2022), [arXiv:2112.04529 \[gr-qc\]](#).
- [49] Víctor Jaramillo, Daniel Martínez-Carbajal, Juan Carlos Degollado, and Darío Núñez, “Born-Infeld boson stars,” *JCAP* **07**, 017 (2023), [arXiv:2303.13666 \[gr-qc\]](#).
- [50] Burkhard Kleihaus, Jutta Kunz, Claus Lammerzahl, and Meike List, “Charged Boson Stars and Black Holes,” *Phys. Lett. B* **675**, 102–115 (2009), [arXiv:0902.4799 \[gr-qc\]](#).
- [51] Sanjeev Kumar, Usha Kulshreshtha, and Daya Shankar Kulshreshtha, “Boson stars in a theory of complex scalar fields coupled to the U(1) gauge field and gravity,” *Class. Quant. Grav.* **31**, 167001 (2014), [arXiv:1605.07210 \[hep-th\]](#).
- [52] Abhay Ashtekar and Anne Magnon-Ashtekar, “On conserved quantities in general relativity,” *Journal of Mathematical Physics* **20**, 793–800 (1979).
- [53] Ericourgoulhon, “An Introduction to the theory of rotating relativistic stars,” in *CompStar 2010: School and Workshop on Computational Tools for Compact Star Astrophysics* (2010) [arXiv:1003.5015 \[gr-qc\]](#).
- [54] Hiroko Niikura *et al.*, “Microlensing constraints on primordial black holes with Subaru/HSC Andromeda observations,” *Nature Astron.* **3**, 524–534 (2019), [arXiv:1701.02151 \[astro-ph.CO\]](#).
- [55] Nolan Smyth, Stefano Profumo, Samuel English, Tesla Jeltema, Kevin McKinnon, and Puragra Guhathakurta, “Updated Constraints on Asteroid-Mass Primordial Black Holes as Dark Matter,” *Phys. Rev. D* **101**, 063005 (2020), [arXiv:1910.01285 \[astro-ph.CO\]](#).
- [56] L. Wyrzykowski *et al.*, “The OGLE View of Microlensing towards the Magellanic Clouds. IV. OGLE-III SMC Data and Final Conclusions on MACHOs,” *Mon. Not. Roy. Astron. Soc.* **416**, 2949 (2011), [arXiv:1106.2925 \[astro-ph.GA\]](#).
- [57] T. Blaineau *et al.*, “New limits from microlensing on Galactic black holes in the mass range $10 M_{\odot} < M < 1000 M_{\odot}$,” *Astron. Astrophys.* **664**, A106 (2022), [arXiv:2202.13819 \[astro-ph.GA\]](#).
- [58] Przemek Mróz *et al.*, “No massive black holes in the Milky Way halo,” *Nature* **632**, 749–751 (2024), [arXiv:2403.02386 \[astro-ph.GA\]](#).
- [59] Przemek Mróz *et al.*, “Limits on Planetary-mass Primordial Black Holes from the OGLE High-cadence Survey of the Magellanic Clouds,” *Astrophys. J. Lett.* **976**, L19 (2024), [arXiv:2410.06251 \[astro-ph.CO\]](#).
- [60] David J. Kaup, “Klein-Gordon Geon,” *Phys. Rev.* **172**, 1331–1342 (1968).
- [61] Sebastien Clesse and Juan García-Bellido, “The clustering of massive Primordial Black Holes as Dark Matter: measuring their mass distribution with Advanced LIGO,” *Phys. Dark Univ.* **15**, 142–147 (2017), [arXiv:1603.05234 \[astro-ph.CO\]](#).
- [62] Bernard Carr, Florian Kuhnel, and Marit Sandstad, “Primordial Black Holes as Dark Matter,” *Phys. Rev. D* **94**, 083504 (2016), [arXiv:1607.06077 \[astro-ph.CO\]](#).
- [63] Gian F. Giudice, Matthew McCullough, and Alfredo Urbano, “Hunting for Dark Particles with Gravitational Waves,” *JCAP* **10**, 001 (2016), [arXiv:1605.01209 \[hep-ph\]](#).
- [64] Víctor Jaramillo, Nicolas Sanchis-Gual, Juan Barranco, Argelia Bernal, Juan Carlos Degollado, Carlos Herdeiro, Miguel Megevand, and Darío Núñez, “Head-on collisions of ℓ -boson stars,” *Phys. Rev. D* **105**, 104057 (2022), [arXiv:2202.00696 \[gr-qc\]](#).
- [65] Mariana Lira, Laura O. Villegas, Javier M. Antelis, Víctor Jaramillo, Claudia Moreno, and Darío Núñez, “On the detectability of gravitational waves emitted from head-on collisions of ℓ -boson stars,” *Gen. Rel. Grav.* **57**, 68 (2025), [arXiv:2411.19401 \[gr-qc\]](#).
- [66] Alfredo Herrera-Aguilar and Ulises Nucamendi, “Kerr black hole parameters in terms of the redshift/blueshift of photons emitted by geodesic particles,” *Phys. Rev. D* **92**, 045024 (2015), [arXiv:1506.05182 \[gr-qc\]](#).
- [67] Chen-Yu Wang, Da-Shin Lee, and Chi-Yong Lin, “Null and timelike geodesics in the Kerr-Newman black hole exterior,” *Phys. Rev. D* **106**, 084048 (2022), [arXiv:2208.11906 \[gr-qc\]](#).
- [68] Laura O. Villegas, Eduardo Ramirez-Codiz, Víctor Jaramillo, Juan Carlos Degollado, Claudia Moreno, Darío Núñez, and Fernando J. Romero-Cruz, “Determination of the angular momentum of the Kerr black hole from equatorial geodesic motion,” *JCAP* **08**, 007 (2023), [arXiv:2211.10464 \[gr-qc\]](#).